CFD ANALYSIS ON LIQUID COOLED COLD PLATE USING COPPER NANOPARTICLES

by

SARTHAK AGARWAL

Presented to the Faculty of the Graduate School of

The University of Texas at Arlington in Partial Fulfilment

of the Requirements for

the Degree of

MASTER OF SCIENCE IN AEROSPACE ENGINEERING

THE UNIVERSITY OF TEXAS AT ARLINGTON

May 2020

Copyright © by Sarthak Agarwal 2020

All Rights Reserved

Acknowledgements

My sincere gratitude goes to Dr.Dereje Agonafer, for giving me the opportunity to work in his EMNSPC Research lab on my thesis research. I would also like to thank him for his encouragement to help me cross all the obstacles and being a true source of inspiration. He has been a constant guiding light and a source of motivation for me and all other members of the lab.

I am thankful to Dr. Miguel Amaya and Dr. Amir Ameri for being a part of my thesis defence committee. I would also like to take this opportunity and thank Pardeep Shahi for being a great team leader on this project. He always motivated and helped me whenever I had doubts about any small things. I thank Satyam Saini for being an amazing team mate in this project. A special thank goes to the industrial mentors of this project, Amirreza Niazmand and Pratik Bhansode for lending me the server, allowing me to do experiments on it and also helping me with valuable inputs and guidance related to the experiments. I would also like to thank my colleagues at the EMNSPC who were as good as my family across seas.

I thank my parents, roommates and friends for their constant moral support throughout my master's degree. Their strength and patience allowed me to focus on my studies and gave me strength to successfully complete my master's degree.

June 05, 2020

Abstract

CFD ANALYSIS ON LIQUID COOLED COLD PLATE USING COPPER NANOPARTICLES

(Reprinted with permission © 2020 ASME)

Sarthak Agarwal, MS

The University of Texas at Arlington, 2020

Supervising Professor: Dr. Dereje Agonafer

In today's world, most data centres have multiple racks with numerous servers in each of them. The high amount of heat dissipation has become the largest server-level cooling problem for the data centres. The higher dissipation required, the higher is the total energy required to run the data centre. Although still the most widely used cooling methodology, air cooling has reached its cooling capabilities especially for High-Performance Computing data centres. Liquid-cooled servers have several advantages over their air-cooled counterparts, primarily of which are high thermal mass, lower maintenance and eventually lower costs by maintenance by labour. Nano-fluids have been used in the past for improving the thermal efficiency of traditional dielectric coolants in the power electronics and automotive industry. Nanofluids have shown great promise in improving the convective heat transfer properties of the coolants due to a proven increase in thermal conductivity and specific heat capacity. The present research investigates the thermal enhancement of the performance of water-based dielectric coolant with Copper nanoparticles for a higher heat transfer from the server cold plates. Detailed 3-D modelling of a commercial cold plate is completed and the CFD analysis is done in a commercially available CFD code ANSYS CFX. The obtained results compare the improvement in heat transfer due to improvement in coolant properties with data available in the literature.

Table of Contents

Acknowledgements iii

Abstract iv

List of Illustrations vi

List of Table……………………………………………………………………………….. vii

Chapter 1 Introduction 8

Chapter 2 Literature Review …………………………………………………………......11

Chapter 3 Numerical Simulation ….……………………………………….…………….…...13

Chapter 4 Geometry, Mesh and Boundary Conditions …......…………….…………….….17

Chapter 5 Results and Discussions ……………………………...…………………….… 21

Chapter 6 Conclusion and Future Work ………………………………………………...27

References 28

Biographical Information 32

List of Illustrations

Figure 1: Traditional Data Centre Cooling Infrastructure, Energy Breakdown ……………8

Figure 2: Full Cold Plate Geometry ………………………………………………………. 17

Figure 3 CoolIT Cold Plate ……………………………………………………………… 18

Figure 4: Cross Section Illustrating the Flow Direction and Heat Source ………………...19

Figure 5: Front Section View……………………………………………………………...19

Figure 6: Dense Mesh at Microchannel …………………...………………………………...20

Figure 7: Mesh of the Fluid Domain……….……………………………………….……….20

Figure 8: Temperature Validation ……………………………………….………………….21

Figure 9: Effects of Volumetric Concentration of Nanoparticles on CPU Temperature ...22

Figure 10: Effects of Volumetric Concentration of Nanoparticles on Pressure Drop ...….23

Figure 11: Effects of Volumetric Concentration of Nanoparticles on Th. Resistance …...24

Figure 12: Temperature Contours For $6cm3/s$ Flow Rate And 0% Concentration …….. 25

Figure 13: Temperature Contours For 6cm3/s Flow Rate And 3% Concentration ..…….25

Figure 14 Temperature Contours For $6cm3/s$ Flow Rate And 5% Concentration……….26

List of Tables

Table 1: Thermal Properties of Nanofluid ……………………………………………….….16

Table 2: Heat sink Dimensions ……………………………………………………………18

Chapter 1

Introduction

Everyday increase in data processing boosts the power consumption for computations by loaded servers. Approximately 2% of the entire power consumption in the United States in 2010 was by data centres. This percentage increased by 8.7% over the years 2011 and 2012 and was expected to increase by 9.8% over the following year. According to a survey, 30% of the electricity consumption in the data centre is utilized by cooling system. [5]

Therefore, better solutions that regulate the amount of cooling required for maintaining energy-efficient device operating temperatures are vital at module, server, and rack-levels.

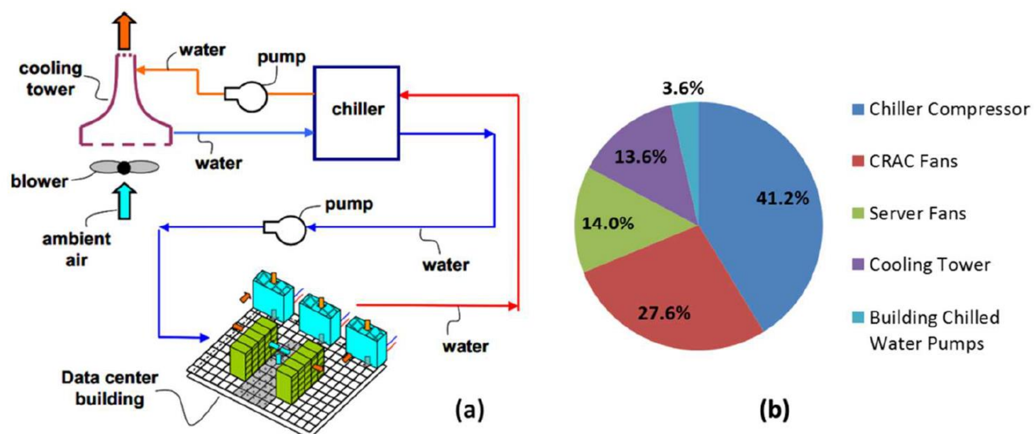

Figure 1: Traditional Data Centre Cooling Infrastructure, Energy Breakdown

Data centres are work spaces specifically dedicated for servers that have an extremely high processing cycle. The size of the work space, i.e. data centre depends on various factors such as number and size of the racks for servers and the area required for the components of the cooling cycle. Servers process very high computations due to which there is a high

amount of heat generated from each processor. This heat needs to be dissipated one way or the other to cool the server and keep it running. The conventional and the most widely used type of cooling used today is air cooling. Ambient air is forced through the channels of the heatsink mounted on each processor for the required dissipation. The fins of the heat sink are carefully designed and simulated such that its maximum area is exposed to the passing air for a higher heat transfer. [2] These simulations are performed on high performance servers using computational Fluid Dynamics (CFD). Various fan sizes are used with respect to the required air flow rate, the amount of heat dissipation required and the available area. Advantages of the air-cooled systems is that the fans used to force the air through the fins do not require a lot of power as compared to liquid cooling which in-turn benefits the operational costs, initial setup costs are low, it has an easier assembly than the liquid-cooled systems and no risk of damage from fluids to the system.

Other type of cooling systems includes oil immersion cooling in which the entire system is immersed in a dielectric fluid. The heat dissipation is directly to the fluid; and vapor chamber in which the fluid is not flowing in the cold plate. For heat transfer, it converts to steam, rises and transfers the heat to the top plate. Vapor chambers are essentially two-phase cooling systems.

Liquid cooling is generally a closed loop system that has a coolant running through pipes. This technology for cooling of servers is comparatively new and has a higher heat transfer rate since conduction is used as the mode of heat transfer. A copper cooling plate with micro-channels is mounted on top of the processor, through which the coolant passes. There is a layer of Thermal Interface Material (TIM) between the copper plate and the processor to improve the thermal coupling between them. There is a heat exchanger such

as a heat exchanger or a radiator at the other end of the loop that dissipates the transferred heat in the coolant. Generally, de-ionized water or other dielectric water-based coolants or such solution is used as the coolant. This coolant flowing in the pipes goes through the channels in the cold plate, absorbs the heat from the processor, flows to the heat exchanger, dissipated the heat and then flows back to the heat source. [22] This entire process requires a higher pumping power than the air-cooled systems. Higher the processor temperatures, higher is the pumping power required. The limitations for liquid cooled systems are there is always a risk of malfunction in the cooling loop with may damage the components, higher number of components for the fluid flow means more chance of component failure, overall energy consumption is higher and the initial setup costs are higher.

In liquid cooling systems, different types of coolants are used based on thermal conductivity and temperature requirements. These coolants include water & ethylene glycol mixtures, Mineral oil and copper oxide or aluminium oxide nanoparticle mixtures. In this paper, de-ionized water is used as the base fluid. For validation, the results of the base fluid are calculated. For increasing the thermal efficiency, the base fluid is injected with different concentrations of copper [22] nanoparticles. The difference in temperature at the cold plate, pressure drop through inlet and outlet and temperature at the outlet are measured and superimposed with the validation readings to get an exact idea of the change in thermal efficiency of the nanofluid as compared to the base fluid.

Chapter 2

Literature Review

2.1 Thermal Analysis of Cold Plate for Direct Liquid Cooling of High-Performance Servers

Data centre energy usage keeps growing every year and will continue to increase with rising demand for ecommerce, scientific research, social networking, and use of streaming video services. By adopting direct liquid cooling, the high heat flux and high-power demands can be met, while the reliability of the electronic devices is greatly improved. Cold plates which are mounted directly on to the chips facilitate a lower thermal resistance path originating from the chip to the incoming coolant. According to [1], an attempt was made in the current study to characterize a commercially available cold plate which uses warm water in carrying the heat away from the chip. The thermo-hydraulic performance of the cold plates was investigated by conducting experiments at varying chip power, coolant flow rates, and coolant temperature. The pressure drop (∇P) and the temperature rise (∇T) across the cold plates were measured, and the results were presented as flow resistance and thermal resistance curves. A maximum of 31 W/cm2 was dissipated at a pressure drop of 4.2 kPa across the cold plates. The thermal resistance of the cold plate was found to decline from 0.056 to 0.029 W/^{o}C as the flow rate increases from 6 to 13 cm3/s indicating a drop in the convective resistance. A heat transfer coefficient of 25 W/cm2K was estimated at the maximum flow rate tested. The experimentally measured pressure drop and cold plate thermal resistance were compared against a numerical mode. An average difference of 8% and 4.5% was observed between the experiments and the model for ∇P and Rcp measurements, respectively.

The thermo-hydraulic performance of the cold plate can be improved by properly understanding the underlying physics and then design the cold plate for optimal pumping power and maximum heat removal. Improving the efficiency at the component level would ultimately enhance the performance of a rack level system.

2.2 Geometric Optimization of an Impinging Cold-Plate Used for Warm Water Cooling

Due to their lower pressure drop, impinging cold-plates are preferred over parallel flow cold-plates when there is no strict space limitation (i.e. when flow can enter perpendicular to the electronic board). Splitting the flow into two branches cuts the flow rate and path in half, which leads to lower pressure drop through the channels. A groove is used to direct the flow exiting the diffuser into the channels. The number of the geometric design parameters of the cold-plate will vary depending on the shape of the groove. The cold plate is used for warm water cooling of electronics. Three fin parameters (thickness, height, and gap) and three groove parameters were optimized to reach minimum values for hydraulic and thermal resistances at fixed values of coolant inlet temperature, coolant flow rate, and electronic chip power. Sensitivity analysis shows that the channel aspect ratio is the most influential parameter for thermal and hydraulic resistances. Finally, it was shown that although groove geometry does not have significant effect on our response parameters, it can affect the temperature profile of the base and electrical die [2].

Chapter 3

Numerical Simulation

3.1 Turbulence Modelling

Eddy Viscosity Models

$$\frac{\partial U_i}{\partial_t} + U_j \frac{\partial U_i}{\partial x_j} = -\frac{1}{\rho}\frac{\partial P}{\partial x_i} + \frac{\partial}{\partial x_j}\left[\frac{(\mu+\mu_t)}{\rho}\frac{\partial U_i}{\partial x_j}\right] \quad (1)$$

These are turbulence models that employ Boussinesq hypothesis, a linear relationship, that is used to model the Reynolds Stresses obtained from the RANS Equations. There are also other non-linear eddy viscosity models that relate thee mean turbulence flow-field to the mean velocity flow-field through the eddy viscosity coefficient. [3]

Classification of Eddy Viscosity Models

- Zero Equation Model (Mixing Length, Cebeci-Smith, Baldwin-Lomax, etc)
- One Equation Model (k Model) (Wolfstein, Baldwin-Barth, Spalart-Allmaras, k-model, etc)
- Two Equation Model (k-ε, k-ω, k-τ, k-L, etc)
- Three Equation Model (k-ε-A)
- Four Equation Model (v2-f model)

Two Equation Model (k-ε Model)

$$\frac{\partial_\epsilon}{\partial t} + U_j \frac{\partial \epsilon}{\partial x_j} = \frac{\epsilon}{k}\left(C_1 \in \frac{\mu_t}{\rho} s^2 - C_{2\epsilon} \in\right) \qquad (2)$$

Two-equation turbulence models allow the determination of both, a turbulent length and time scale by solving two separate transport equations.

The standard model is a model based on model transport equations for the turbulence kinetic energy (k) and its dissipation rate (ε). The model transport equation for (k) is derived from the exact equation, while the model transport equation for (ε) was obtained using physical reasoning and bears little resemblance to its mathematically exact counterpart. In the derivation of the - model, the assumption is that the flow is fully turbulent, and the effects of molecular viscosity are negligible. The standard model is therefore valid only for fully turbulent flows. In this study, standard κ-ε model was used to model kinetic energy and turbulent dissipation.

Flow Equations

- Continuity equation

$$\frac{\partial \rho}{\partial_t} + \nabla \cdot (\rho U) = 0 \qquad (3)$$

- Momentum Equation

$$\frac{\partial}{\partial t}(\rho U) + \nabla \cdot (\rho U U) = -\nabla_P + \nabla_\tau + B \qquad (4)$$

- Energy equation

$$\frac{\partial}{\partial t}(\rho h) + \nabla \cdot (\rho U C_P T) = \nabla \cdot (k \nabla T) \quad (5)$$

3.2 Basic assumptions applied to the simulation

The flow is three-dimensional, steady, laminar, and Incompressible. The effects of gravity are negligible. The thermo-physical properties like conductivity, specific heat, viscosity of the coolant, and solid phases are constant. Viscous heating and radiation heat transfer are omitted.

3.3 Calculation of Nanofluid Properties

- Density

$$\left(\rho_{nf}\right) = (1-\phi)_{\rho_f} + \phi\rho_s \quad (6)$$

- Specific Heat

$$\left(\rho c_p\right)nf = (1-\phi)(\rho Cp)_f + \phi(\rho Cp)s \quad (7)$$

- Viscosity

$$\mu_{nf} = \mu_f (1-\phi)^{-2\cdot 5} \quad (8)$$

- Thermal Conductivity

$$K_{nf} = k_f \left[\frac{k_s+2k_f-2\phi(k_f-k_s)}{k_s+2k_f+\phi(k_f-ks)}\right] \quad (9)$$

Volume Concen-tration (%)	Density $(\mathrm{kg/m^3})$	Specific Heat $(\mathrm{J/kgK})$	Thermal Conductivity $(\mathrm{w/mK})$	Viscosity $(\mathrm{kg/ms})$
0	998.2	4182	0.6	0.001003
3	1237.6	3355.24	0.6554	0.001082
5	1397.2	2961.46	0.6743	0.00114

The equations (6,7,8,9) are used to determine the density, specific heat, viscosity and thermal conductivity of the nanofluid for the simulation at different concentrations. As the volumetric concentration of the nanoparticle increases, the density increases, specific heat decreases, thermal conductivity increases, and the viscosity also increases. [3]

Chapter 4

Geometry, Mesh and Boundary Conditions

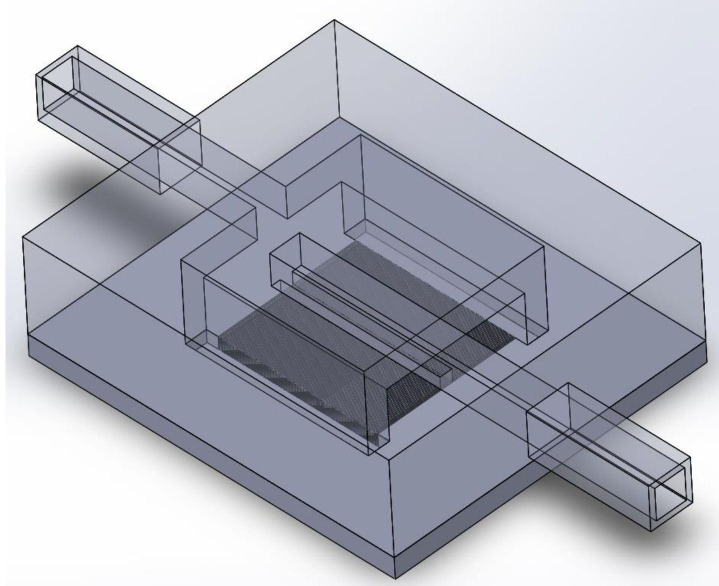

Figure 2: Full Cold Plate Geometry

The 3D geometry of the cold plate designed in SolidWorks is shown in Figure 2, i.e. the complete assembly, including the copper plate (grey), the top cover (transparent) and the fluid domain. Boundary conditions are that the heat source is defined at the bottom of the copper plate, illustrating a processor. The coolant flow velocity and temperature are specified at the inlet. Static pressure conditions are defined at the outlet. The surfaces of the top cover are assumed to be adiabatic. The dimensions of the fins and channels are the same as the experimental setup used by [1].

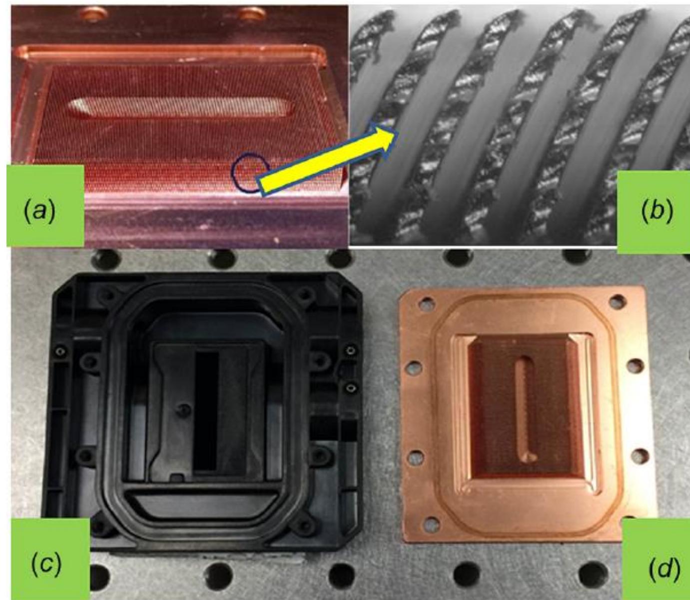

Figure 3: CoolIT Cold Plate [1]

The design of the microchannels have been modelled after the Cool IT cold plates which are show in this image. B is the zoomed in image of the microchannels and C is the non-conductive top portion of the cold plate; while D is the copper plate with microchannels.

Heat sink dimensions	
Length of channel	31.52mm
Breath of channel	23.56mm
Thickness of fin	100.6 µm
Channel width	154.3 µm
Height of fin	2.02mm
Thickness of base	1.35mm

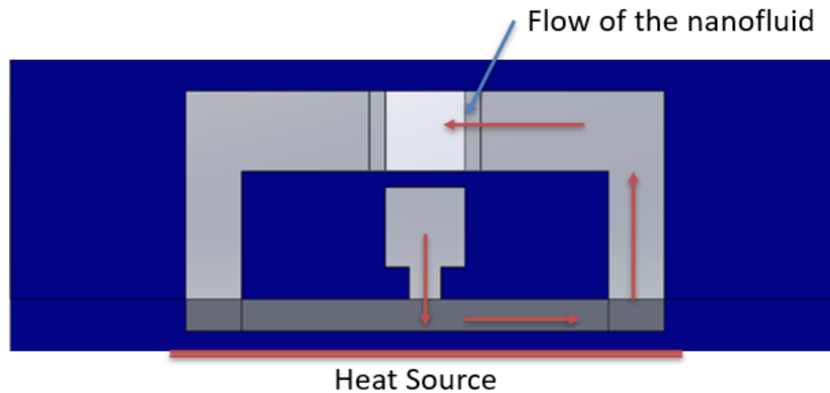

Figure 4: Cross Section Illustrating the Flow Direction and Heat Source

The heat source is located at the bottom of the cold plate highlighted in red in the bottom image, where the heat flux is given. The heat source is modelled after an actual processor dimension. The bottom plate is made from pure copper and the top transparent portion of the plate is made from a non-conducting material such as plastic or rubber.

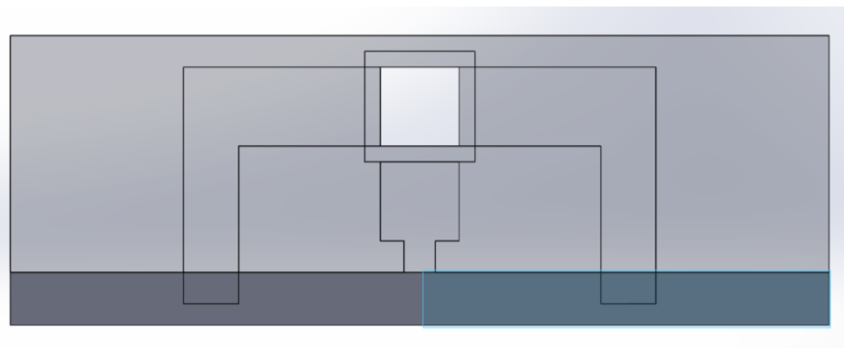

Figure 5: Front Section View

Figure 3 illustrates the sectional front view of the geometry. For simulation purpose, one microchannel is considered. This enables creating a dense mesh at the area of observation, i.e. one microchannel. The blue section at the bottom right is the half fin that is considered for the simulation.

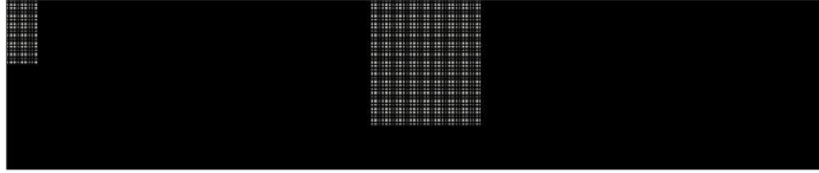

Figure 6: Dense Mesh at Microchannel

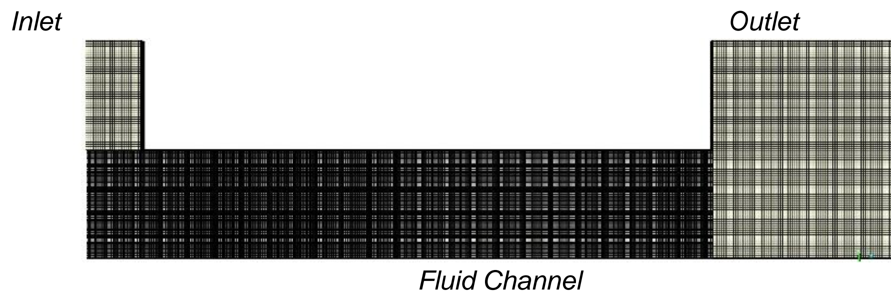

Figure 7: Mesh of The Fluid Domain

Mesh Density governs the accuracy of the results which is why it was vital to have such high number of elements and nodes. Figure 4 represents one microchannel and Figure 5 represents the fluid domain in that microchannel. One fin is considered for the simulation instead of the entire geometry because the validation results for the base fluid achieved for both cases were similar. In order to reduce the computational time, it was decided to consider single fin for all simulations. The fluid enters through the inlet, flows between two adjacent fins and then exits through the outlet. At the inlet, Mass-flow-Rate boundary condition is used. The magnitude of the mass-flow rate is specified in kg/s at the direction that is normal to the boundary. At the outlet, the boundary condition used is outflow. The static pressure is specified at the outlet. Along with the energy equation, k-ε Model is used as the turbulence equations.

Chapter 5

Results and Discussions

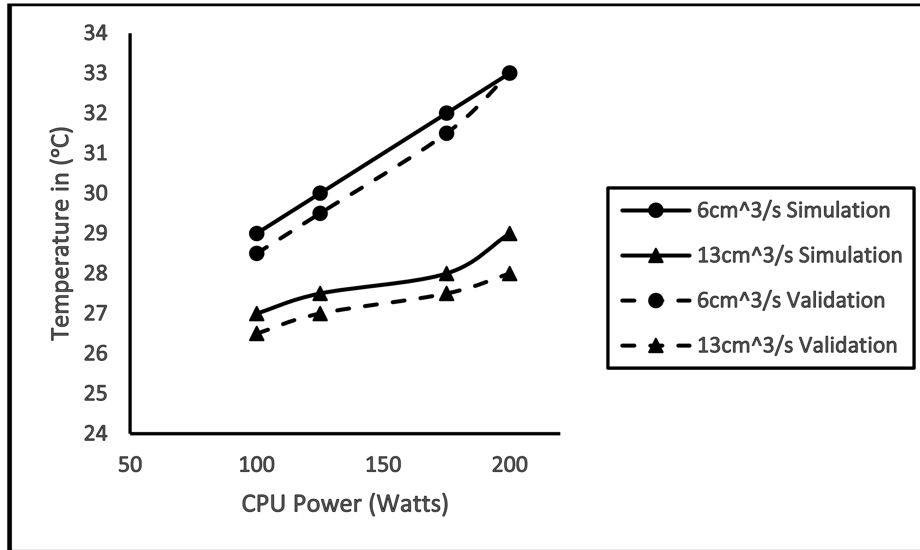

***Figure 8**: Temperature Validation [1]*

Figure 8 illustrates the graph that validates the temperature results at the outlet of the cold plate. The dotted lines are the temperature plots taken from the reference paper and the solid lines are the simulation results. The simulations for both were performed at 100W, 125W, 175W and 210W with 6cm3/s and 13 cm3/s inlet volumetric flow rates. It is observed that there is a temperature difference of almost 0.5°C in the validation and simulation results which can be neglected.

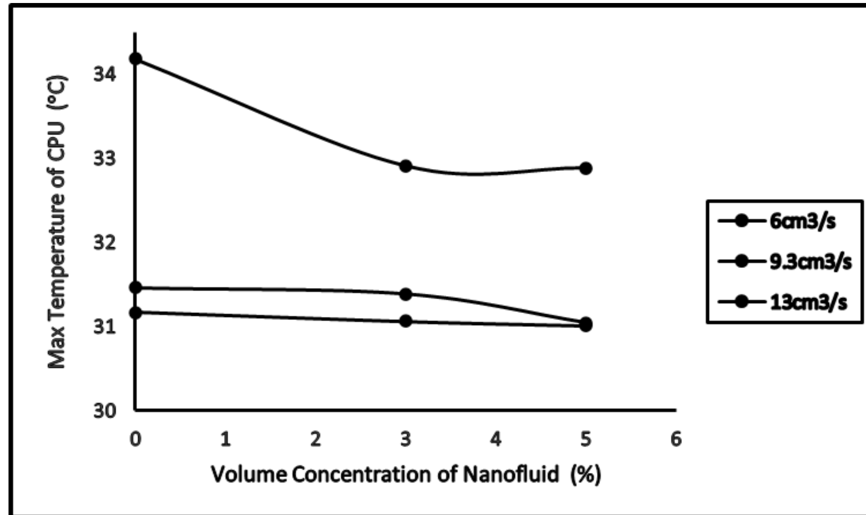

Figure 9*: Effects of Volumetric Concentration of Nanoparticles on CPU Temperature*

Thermal conductivity is the factor due to which there is heat transfer from the walls to the liquid whereas Heat Capacity is the parameter which enables the fluid to carry the heat. When increasing the nanoparticles concentration in the fluid, the thermal conductivity of the nanofluid is increased but the heat capacity is decreased. This is because the heat capacity of metals is less than that of fluids. Therefore, there is an optimum value of the volume concentration of the nanoparticles that can be added. Hence, in Figure 9, the temperature at the CPU decreases when the flow is at 6cm^3/s and the concentration of nanoparticles changes from 0% to 3% and the temperature remains constant when the concentration changes from 3% to 5%.

The heat transfer in this case is based on convection. For a high velocity, the gradient of temperature close to the walls becomes very high. Therefore, it is difficult to detect the effects of thermal conductivity. This is why when the flow rate is increased to 9.3cm^3/s and 13cm^3/s, the temperature remains constant.

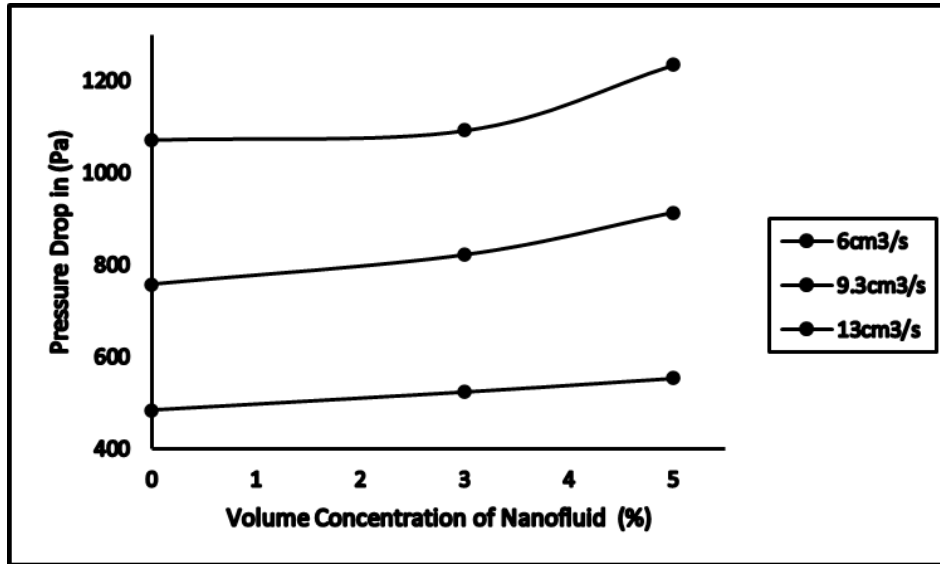

Figure 10*: Effects of Volumetric Concentration of Nanoparticles on Pressure Drop*

The flow rate is directly proportional to the velocity of the fluid. Hence, when the pressure is increased for a constant geometry, the flow rate also increases. Similarly, when the flow rate is increased, the pressure increases respectively because of a higher flow passing through the same dimension. The same thing is taking place in Figure 10. The Pressure drop is increasing as the flow rate is increasing. We can also notice that when the concentration of the nanoparticles is increased, there is no significant change in the pressure drop across the system.

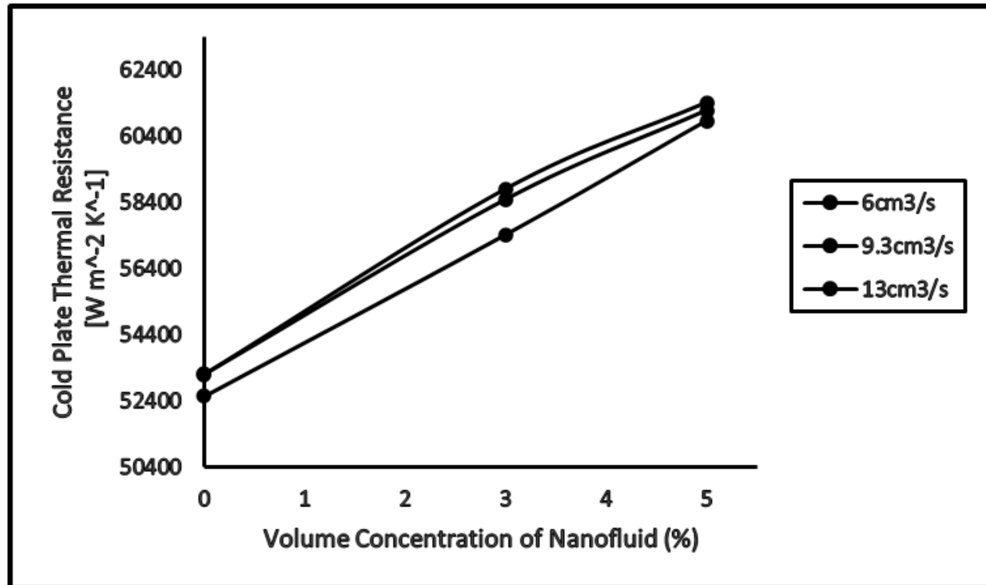

***Figure 11**: Effects of Volumetric Concentration of Nanoparticles on Thermal Resistance*

Thermal resistance is the ratio of the temperature difference between the two faces of a material to the rate of heat flow per unit area. It determines the resistance of heat transfer in material. As the thermal resistance increases, the heat loss decreases. The thermal conductivity of a solid is lower than fluid. Hence, when solid nanoparticles are added to the fluid, the thermal resistance of the material increases.

In Figure 11, the thermal resistance increases by 7.6% when the concentration of nanoparticles changes from 0% to 3% and it increases by 7.2% when the concentration changes from 3% to 5%. This trend follows irrespective of the flow rate.

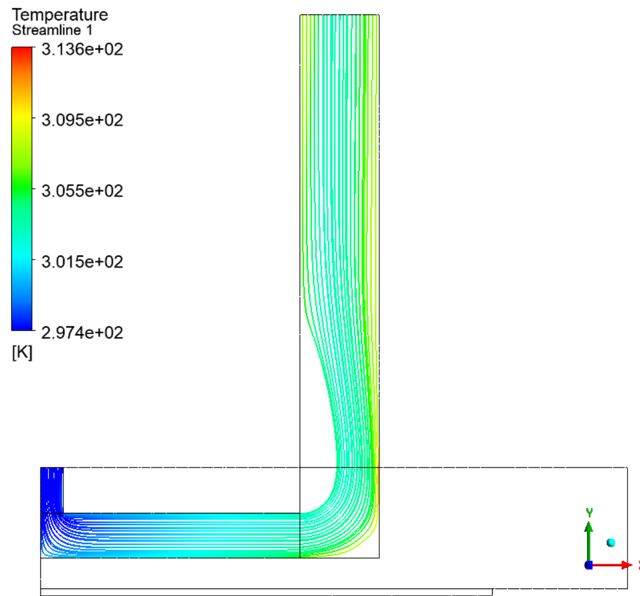

***Figure 12**: Temperature Contours For*
6CM^3/S Flow Rate And 0% Concentration

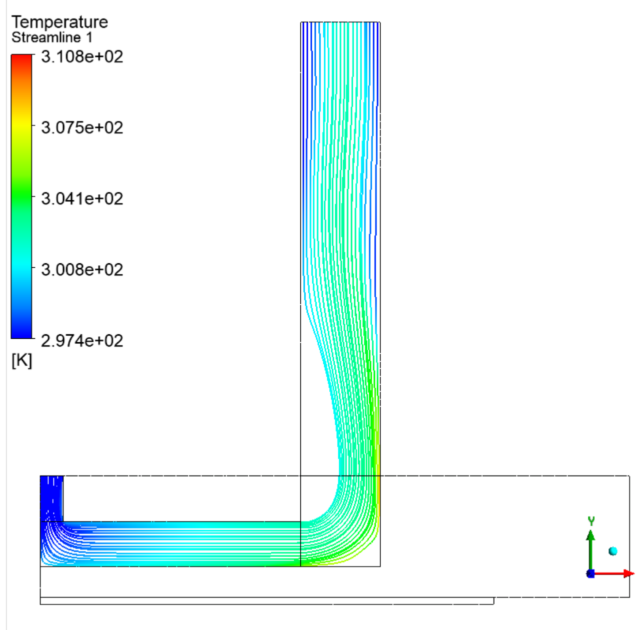

***Figure 13**: Temperature Contours For*
6CM^3/S Flow Rate And 3% Concentration

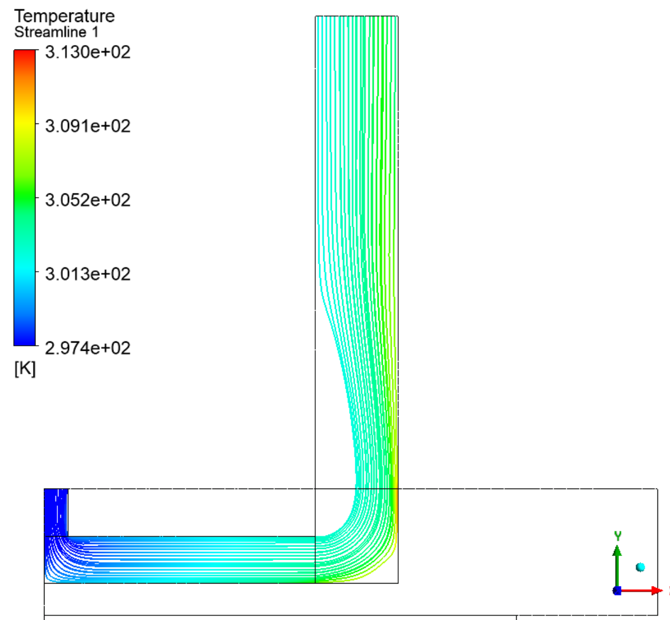

***Figure 14**: Temperature Contours For*
6Cm^3/S Flow Rate And 5% Concentration

The Figures 12, 13 and 14 represent the streamlines for flow at 6cm3/s and a nanoparticle concentration of 0%, 3% and 5% respectively. The coolant enters the system from the inlet on the left, flows through the microchannels and exits through the outlet on the top side of the geometry. It is observed that there is a significant flow separation when the direction of the flow changes. This results in a pressure drop across the system. Therefore, to reduce the pressure drop, the geometry of the cold plate can further be improved.

Chapter 6

Conclusion and Future Work

According to the observations of the results, it is clear that when the concentration of the nanoparticles increases more than 3%, the temperature drop with respect to the pressure drop is not very high. Thus, we can conclude that a 3% concentration of copper nanoparticles in a base fluid of water is optimal. To have a better understanding of the nanofluid, simulations need to be performed with lower flow rates and higher inlet temperature, because at a lower inlet flow, the heat transfer to the fluid is higher and at higher temperatures, a better estimation of the cold plate functionality can be studied. To further reduce the pressure drop across the system, the geometry of the cold plate can be improved.

Also, on the base of cold plate temperature, an automated flow control valve can be used to control the mass flow rate. This will further reduce the overall cost of each server and in turn, the data centres.

The issue of contamination related failures limit air cooling techniques to be successfully implemented for data centres looking to lower their PUE. While it’s true that air cooling will continue to dominate the data centre cooling industry, especially for enterprise storage systems, and latest phase change and direct immersion cooling techniques are also being used for cooling high performance clusters, indirect liquid cooling presents the simplest and the best option for cooling high heat fluxes without significant changes to existing data centre infrastructure [23-30].

References

[1] Bharath Ramakrishnan, Yaser Hadad “Thermal Analysis of Cold Plate for Direct Liquid Cooling of High Performance Servers” ASME Journal 041005-6 / Vol. 141, DECEMBER 2019

[2] Yaser Hadad*, Reza Pejman, “Geometric Optimization of an Impinging Cold-Plate with a Trapezoidal Groove Used for Warm Water Cooling” 17th IEEE ITHERM Conference

[3] Simulation of Turbulent Flows, web.stanford, ME469B/3/GI

[4] Dereje Agonafer, Vinod Kamath, “Multi-Design Variable Optimization for a Fixed Pumping Power of a Water-Cooled Cold Plate for High Power Electronics Applications” 13th IEEE ITHERM Conference

[5] Arman Shehabi, Sarah Josephine Smith https://eta.lbl.gov/publications/united-states-data-center-energy

[6] Tonapi, S. S., Fillion, R. A., Schattenmann, F. J., Cole, H. S., Evans, J. D., and Sammakia, B. G., 2003, “An Overview of Thermal Management for Next Generation Microelectronic Devices,” Advanced Semiconductor Manufacturing Conference and Workshop, IEEEI/SEMI (ASMC), Munich, Germany, Mar. 31–Apr. 1, pp. 250–254.

[7] Chu, R. C., Bar-Cohen, A., Edwards, D., Herrlin, M., Price, D., Schmidt, R., and Sammakia, B., 2003, “Thermal Management Roadmap Cooling Electronic Products From Handheld Device to Supercomputers,” MIT Rohsenow Symposium, Cambridge, MA, May 16.

[8] Alkharabsheh, S., Fernandes, J., Gebrehiwot, B.,Agonafer, D., Ghose, K., Ortega, A., Joshi, Y., and Sammakia, B., 2015, “A Brief Overview of Recent Developments in Thermal Management in Data Centers,” ASME. J. Electron. Packag., 137(4), p. 040801.

[9] Ellsworth, M. J., Jr., and Iyengar, M. K., 2009, “Energy Efficiency Analyses and Comparison of Air and Water Cooled High Performance Servers,” ASME Paper No. InterPACK2009-89248.

[10] David, M., Iyengar, M., Parida, P., Simons, R., Schultz, M., Gaynes, M., Schmidt, R., and Chainer, T., 2012, “Experimental Characterization of an Energy Efficient Chiller-Less Data Center Test Facility With Warm Water Cooled Servers,” 28th Annual IEEE Semiconductor Thermal Measurement and Management Symposium (SEMI-THERM), San Jose, CA, Mar. 18–22, pp.
232–237.

[11] Ebrahimi, K., Jones, G. F., and Fleischer, A. S., 2014, “A Review of Data Center Cooling Technology, Operating Conditions and the Corresponding Low- Grade Waste Heat Recovery Opportunities,” Renewable Sustainable Energy Rev., 3, pp. 622–638.

[12] Ebrahimi, K., Jones, F., and Fleischer, A. S., 2015, “Thermo-Economic Analysis of Steady State Waste Heat Recovery in Datacenters Using Absorption Refrigeration,” Appl. Energy, 139, pp. 384–397.

[13] Araya, S., Jones, G. F., and Fleischer, A. S., 2016, “The Design and Construction of a Bench-Top Organic Rankine Cycle for Data Center Applications,” ITherm 2016, Las Vegas, NV, Paper No. 167.

[14] Tuckerman, D. B., and Pease, R. F. W., 1981, “High-Performance Heat Sinking for VLSI,” IEEE Electron Device Lett., 2(5), pp. 126–129. [13] Knight, R. W., Hall, D. J., Goodling, J. S., and Jaeger, R. C., 1992, “Heat Sink Optimization with Application to Microchannels,” IEEE Trans. Compon. Hybrids Manuf. Technol., 15(5), pp. 832–842.

[15] Copeland, D., 2000, “Optimization of Parallel Plate Heatsinks for Forced Convection,” 16th Annual IEEE Semiconductor Thermal Measurement and Management
Symposium, San Jose, CA, Mar. 23, pp. 266–272.

[16] Chiu, H.-C., Jang, J.-H., Yeh, H.-W., and Wu, M.-S., 2011, “The Heat Transfer Characteristics of Liquid Cooling Heatsink Containing Microchannels,” Int. J. Heat Mass Transfer, 54(1–3), pp. 34–42.

[17] Lee, P.-S., Garimella, S. V., and Liu, D., 2005, “Investigation of Heat Transfer in Rectangular Microchannels,” Int. J. Heat Mass Transfer, 48(9), pp. 1688–1704.

[18] Zhang, H. Y., Pinjala, D., Wong, T. N., Toh, K. C., and Joshi, Y. K., 2005, “Single-Phase Liquid Cooled Microchannel Heat Sink for Electronic Packages,” Appl. Therm. Eng., 25(10), pp. 1472–1487.

[19] Alkharabsheh, S., Ramakrishnan, B., and Sammakia, B., 2017, “Pressure Drop Analysis of Direct Liquid Cooled (DLC) Rack,” 16th IEEE Intersociety Conference on Thermal and Thermomechanical Phenomena in Electronic Systems (ITherm), Orlando, FL, May 30–June 2, pp. 815–823.

[20] Lee, S., Song, S., Au, V., and Moran, K. P., 1995, “Constriction/Spreading Resistance Model for Electronic Packaging,” Fourth ASME/JSME Thermal Engineering Joint Conference, Maui, HI, Mar 19–24, pp. 199–206.

[21] Mills, M. P., 2013, “The Cloud Begins With Coal,” Tech-Pundit, accessed July 2, 2019, http://www.techpundit.com/wpcontent/uploads/2013/07/Cloud_Begins_With_Coal.pdf?c761ac

[22] M.RafatiA.A.Hamidi, “Application of nanofluids in computer cooling systems (heat transfer performance of nanofluids)” Applied Thermal Engineering Volumes 45–46, December 2012, Pages 9-14
[23] Jimil M. Shah, Chinmay Bhatt, Pranavi Rachamreddy, Ravya Dandamudi, Satyam Saini, Dereje Agonafer, 2019, Computational Form Factor Study of a 3rd Generation Open Compute Server for Single-Phase Immersion Cooling, ASME Conference Paper No. IPACK2019-6602

[24] Dhruvkumar Gandhi, Uschas Chowdhury, Tushar Chauhan, Pratik Bansode, Satyam Saini, Jimil M. Shah and Dereje Agonafer, 2019, Computational analysis for thermal optimization of server for single phase immersion cooling, ASME Conference Paper No. IPACK2019-6587

[25] Pravin A Shinde, Pratik V Bansode, Satyam Saini, Rajesh Kasukurthy, Tushar Chauhan, Jimil M Shah and Dereje Agonafer, 2019, Experimental analysis for optimization of thermal performance of a server in single phase immersion cooling, ASME Conference Paper No. IPACK2019-6590

[26] Jimil M. Shah, Roshan Anand, Satyam Saini, Rawhan Cyriac, Dereje Agonafer, Prabjit Singh, Mike Kaler, 2019, Development of A Technique to Measure Deliquescent Relative Humidity of Particulate Contaminants and Determination of the Operating Relative Humidity of a Data Center, ASME Conference Paper No. IPACK2019-6601

[27]Gautham Thirunavakkarasu, Satyam Saini, Jimil Shah, Dereje Agonafer,2018, Airflow pattern and path flow simulation of airborne particulate contaminants in a high-density Data Center utilizing Airside Economization, ASME Conference Paper No. IPACK2018-8436

[28] Kumar, A., Shahi, P., & Saha, S. K. Experimental Study of Latent Heat Thermal Energy Storage System for Medium Temperature Solar Applications.

[29] Saini, Satyam. Airflow Path and Flow Pattern Analysis of Sub-Micron Particulate Contaminants in a Data Center with Hot Aisle Containment System Utilizing Direct Air Cooling. Diss. 2018.

[30] Dehkordi, B. G., Fallah, S., & Niazmand, A. (2014). Investigation of harmonic instability of laminar fluid flow past 2D rectangular cross sections with 0.5–4 aspect ratios. Proceedings of the Institution of Mechanical Engineers, Part C: Journal of Mechanical Engineering Science, 228(5), 828–839. https://doi.org/10.1177/0954406213491906

Biographical Information

Sarthak has received his Master of Science degree in Aerospace Engineering from The University of Texas at Arlington. He completed his Bachelor of Technology in Mechanical Engineering from Mukesh Patel School of Technology Management and Engineering, India. He had been working in the EMNSPC Research lab at UTA on liquid cooling of the server and CFD analysis of the server.